

## Supplementary Information for

### Semaphorin signaling via MICAL3 induces symmetric cell division to expand breast cancer stem-like cells

Kana Tominaga<sup>a,b,c\*</sup>, Hiroshi Minato<sup>d†</sup>, Takahiko Murayama<sup>a</sup>, Asako Sasahara<sup>a,e</sup>, Tatsunori Nishimura<sup>c</sup>, Etsuko Kiyokawa<sup>d</sup>, Hajime Kanauchi<sup>f</sup>, Seiichiro Shimizu<sup>g</sup>, Ayaka Sato<sup>e</sup>, Kotoe Nishioka<sup>e</sup>, Ei-ichi Tsuji<sup>e</sup>, Masao Yano<sup>h</sup>, Toshihisa Ogawa<sup>f</sup>, Hideshi Ishii<sup>i</sup>, Masaki Mori<sup>j</sup>, Koichi Akashi<sup>k</sup>, Koji Okamoto<sup>b</sup>, Masahiko Tanabe<sup>e</sup>, Kei-ichiro Tada<sup>e‡</sup>, Arinobu Tojo<sup>a</sup> and Noriko Gotoh<sup>a,c</sup>

#### Affiliations

- a. Division of Molecular Therapy, Institute of Medical Science, University of Tokyo,  
Minato-ku, Tokyo, 108-8639, Japan
- b. Division of Cancer Differentiation, National Cancer Center Research Institute,  
Chuo-ku, Tokyo, 104-0045, Japan
- c. Division of Cancer Cell Biology, Cancer Research Institute, Kanazawa University,  
Kanazawa city, Ishikawa, 920-1192, Japan
- d. Department of Pathology and Laboratory Medicine, Kanazawa Medical University,  
Uchinada-machi, Ishikawa, 920-0265, Japan
- e. Department of Breast and Endocrine Surgery, Graduate School of Medicine,  
University of Tokyo, Bunkyo-ku, Tokyo, 112-8655, Japan
- f. Department of Breast and Endocrine Surgery, Showa General Hospital, Kodaira

city,

Tokyo, 187-8510, Japan

- g. Department of Pathological Diagnosis, Showa General Hospital, 8-1-1 Hanakoganei, Kodaira city, Tokyo, 187-8510, Japan
- h. Department of Surgery, Minami-machida Hospital, Machida-city, Tokyo, 194-0004, Japan
- i. Department of Medical Data Science, Osaka University Graduate School of Medicine, Suita-city, Osaka, 565-0871, Japan
- j. Department of Gastroenterological Surgery, Graduate School of Medicine, Osaka University, Suita-city, Osaka, 565-0871, Japan
- k. Department of Medicine and Biosystemic Science, Graduate School of Medical School, Kyushu University, Fukuoka, 812-8582, Japan

\*Present address: Department of Biology, Massachusetts Institute of Technology, Cambridge, MA 02139, USA

†Present address: Department of Diagnostic Pathology, Ishikawa Prefectural Central Hospital, Kanazawa city, 920-8530, Japan

‡Present address: Department of Breast Surgery, National Center for Global Health and Medicine, Shinjuku-ku, 162-8655, Japan

**Classification: Biological Sciences, Medical Sciences**

**Short title: MICAL3 for symmetric division of cancer stem cells**

**Corresponding authors:**

Noriko Gotoh, MD, PhD

Professor

Division of Cancer Cell Biology

Cancer Research Institute, Kanazawa University

Kakuma-machi, Kanazawa City, Ishikawa 920-1192, Japan

Phone: 81-76-264-6730; Fax: 81-76-234-4517

Email: [ngotoh@staff.kanazawa-u.ac.jp](mailto:ngotoh@staff.kanazawa-u.ac.jp), [ngotoh@ims.u-tokyo.ac.jp](mailto:ngotoh@ims.u-tokyo.ac.jp)

&

Kana Tominaga, PhD

Postdoctoral fellow  
Division of Molecular Therapy,  
Institute of Medical Science, The University of  
Tokyo 4-6-1 Shirokanedai, Minato-ku, Tokyo 108-  
8639, Japan

Phone: 81-3-5449-5551, FAX: 81-3-5449-5425

Email: k.n.tominaga22@gmail.com

**This PDF file includes:**

Supplementary text  
Figs. S1 to S23  
Tables S1 to S4  
References for SI reference citations

**Supplementary Information Text**

**Materials and Methods**

**Culture of Cell Lines**

The mammary epithelial cell line, MCF10A, and the breast cancer cell lines, MCF7, T47D, BT20, BT474, and MDA-MB-436, were purchased from the American Type Culture Collection. Cells were cultured in RPMI 1640 culture medium (Nacalai Tesque) containing 10% fetal bovine serum (SAFC Biosciences), 100 units/ml penicillin, and 100 µg/ml streptomycin (Nacalai Tesque). Cell lines were cultured in a humidified atmosphere at 37°C in 5% CO<sub>2</sub>, and the culture medium was changed every 2 days. When cells reached subconfluence, they were rinsed in phosphate-buffered saline (PBS) (pH 7.4, Nacalai Tesque), trypsinized with 0.25% Trypsin-EDTA Solution (Nacalai Tesque) for 1 min at 37°C, and passaged at ratios of 1:3 to 1:5. Cell proliferation was analyzed by MTT assay kit (Sigma).

**Isolation of Single Cells from Breast Tumor Tissues**

Patient-derived tumor tissues were cut into <5 mm<sup>3</sup> pieces in PBS. A mechanical disaggregation system (Medimachine, Becton Dickinson) was used to obtain single-cell suspensions from the solid tumors. A Medicon (50 µm) device containing the tissues was inserted into the Medimachine (BD™ Medimachine) and subjected to a 1-min pulse. The resulting single-cell suspension was filtered through a 100-µm cell strainer (BD Falcon) and washed with PBS. In the case of disaggregated cell clusters, the single-cell suspension was incubated in Accumax (Innova Cell Technologies) at room temperature for 10 min.

**Primary Cell Culture**

To isolate Lin<sup>-</sup> breast cancer cells, cells obtained from breast tumor specimens were incubated with a mixture of biotin-conjugated antibodies against Lin<sup>+</sup> cells as previously described (10). The antibody mixture included a magnetic cell separation (MACS) lineage kit for depletion of hematopoietic and erythrocyte precursor cells (CD2, CD3, CD11b, CD14, CD15, CD16, CD19,

CD56, CD123, and CD235a, Miltenyi Biotec), endothelial cells (CD31, eBioscience), and stromal cells (CD140b, Biolegend). After incubation, cells were separated using the MACS system according to the manufacturer's instructions (Miltenyi Biotec). Isolated lineage-negative (Lin<sup>-</sup>) breast cancer cells were cultured in Human EpiCult™-B Medium Kit medium (Stem Cell Technologies) that includes a supplement mix, freshly prepared 0.48 µg/ml hydrocortisone (Stem Cell Technologies), 2 mM L-glutamine (Nacalai Tesque), 100 units/ml penicillin, and 100 µg/ml streptomycin. Isolated single cells were cultured in a humidified atmosphere at 37°C in 5% CO<sub>2</sub>, and the culture medium was changed every 2 days. When cells reached subconfluence, they were rinsed in PBS, trypsinized with Accumax for 10 min at room temperature, and passaged at a ratio of 1:4.

### **Tumor Sphere Formation Assay**

We previously confirmed that patient-derived breast cancer cells plated at 5,000 cells/ml yield tumor spheres that are clonally derived from single cell (8). Cells were therefore plated as single cell suspensions in 24-well or 96-well ultra-low attachment plates at a low density (5,000 cells/ml) to obtain single cell-derived tumor spheres. The cells were grown in SCM, which consists of serum-free Dulbecco's modified Eagle's Medium: Nutrient Mixture F-12 (DMEM/F-12) medium (GIBCO), 20 ng/ml epidermal growth factor (Millipore), 20 ng/ml basic fibroblast growth factor (PeproTech), B27 supplement (GIBCO), and 2 µg/ml heparin (Stem Cell Technologies), as previously described (10). Alternatively, spheres were grown in DMEM/F-12 medium supplemented with 200 ng/ml recombinant human Sema3A (R&D Systems Inc.), anti-NP1 antibody or control IgG (R&D Biosystems). Spheres with a diameter >75 µm were counted after 4 to 7 days.

### **Construction of Lentivirus Vectors**

The pENTR4-H1 vector containing the shRNA sequence (100 µg) and a lentiviral vector (150 ng/µl) (CS-RfA-EG) were used for recombination with a Gateway® LR Clonase® Enzyme mix (Invitrogen) containing proteinase K according to the manufacturer's recommendations, to generate the shRNA expression clone. Lentivirus plasmid DNA (1000 ng/µl) was transduced into HEK293FT cells along with packaging plasmids (pCMV-VSV-G-RSV-Rev and pCAGHIVgp) using the lipofectamine transfection reagent (Invitrogen) and PLUS™ Reagent (Invitrogen). The medium was changed after 16 hr. High-titer viral stocks were prepared by ultracentrifugation.

### **shRNA and siRNA**

For construction of the lentivirus plasmid vector for knockdown of *MICAL3*, the shRNA sequence (Table S2) was inserted in the pENTR4-H1 vector (a kind gift from H. Miyoshi, RIKEN, Tsukuba, Japan) as an entry vector. siRNAs for *MICAL3* were purchased from GE Healthcare (Catalog number LU-024432-00-0002) (Table S3). siRNAs for *CRMP2*, or *Numb* were purchased from Invitrogen (Table S4).

### **Transduction of Cells with Lentiviral Vectors**

The culture supernatant containing infection-competent virus particles was applied to cultivated MCF7 cells or patient-derived breast cancer cells at a multiplicity of infection of 1:10, and was incubated for 24 hr at 37°C in 5% CO<sub>2</sub>. After incubation, GFP-positive cells were sorted using fluorescence-activated cell sorting (FACS) Aria II (BD Bioscience).

### **Knockdown experiments by using siRNAs**

For knockdown of *MICAL3*, breast cancer cell lines (MCF7 and BT20) or patient-derived breast cancer cells were seeded at a density of  $3 \times 10^5$  cells/well into a 6-well plate. After incubation for 24 hr, cells were incubated with ON-TARGETplus *MICAL3* siRNA and DharmaFECT transfection reagent (GE Healthcare) in serum-free medium. The control was an ON-TARGETplus non-targeting siRNA. For knockdown of *CRMP2* and *Numb*, breast cancer cell lines (MCF7 and BT20) were seeded at a density of  $5 \times 10^5$  cells/well into a 6-well plate and incubated with Stealth RNAi™ (Invitrogen) and Lipofectamine™ RNAiMAX transfection reagent (Invitrogen) according to the manufacturer's protocol. RNAi duplex (10 nM final concentration) and Lipofectamine™ RNAiMAX complexes were added to each well. The control was the Stealth™ RNAi Negative Control with low GC content. siRNA-transfected cells were incubated at 37°C in 5% CO<sub>2</sub> until the assay. Representative data from three independent experiments using two types of siRNAs are shown.

### **Transient Transfection with Plasmids**

We used the following described expression vectors: GFP-MICAL3, GFP-MICAL3-3G3W, and GFP-MICAL3-N1 (3). The control was a pEGFP-C1 vector. GFP-MICAL3 was generated from the human cDNA clone, pF1KA0819, using a modified pEGFP-C1 vector. GFP-MICAL3-3G3W and GFP-MICAL3-N1 were generated from GFP-MICAL3 using a PCR-based strategy. The control was a pEGFP-C1 vector. For transient transfection of plasmids, cells were seeded at a density of  $3 \times 10^5$  cells/well into a 6-well plate. After incubation for 24 hr, the plasmids (1.8 µg) and a PolyFect Transfection Reagent (Qiagen) in culture medium without antibiotics were added to each well.

### **Flow Cytometry**

To analyze the population of BCSCs, single cells were sorted after staining with Alexa flour 647-labeled anti-CD24 (BD Biosciences) and APC-H7-labeled anti-CD44 (BD Biosciences) antibodies. As isotype controls, Alexa flour 647-labeled mouse IgG2a and APC-H7-labeled mouse IgG2b (BD Biosciences) antibodies were used. To analyze receptors for Sema3A, anti-NP1 (446921, R&D Biosystems) antibodies or anti-Plexin A4 (MM087416T23, abcam) at 4°C for 20 min. After washing with PBS, cells were incubated with Alexa 488 anti-rabbit IgG antibody or Alexa 546 anti-goat IgG antibody as a secondary antibody at 4°C for 20 min. Dead cells were excluded using propidium iodide (Nacalai Tesque) staining. All flow cytometric analyses were performed with a FACS Aria II (BD Bioscience), and data were analyzed using FlowJo software (Treestar).

### **Immunoblotting**

For SDS-PAGE, cultured cells in 6-well plates were washed with PBS and then lysed with Lysis buffer containing RIPA Buffer (Pierce), a Phosphatase Inhibitor Cocktail (Nacalai Tesque), and a Protease Inhibitor Cocktail (Nacalai Tesque) as previously described (10). For non-reducing SDS-PAGE, the cells were lysed in a buffer containing 15 mM iodoacetamide (Sigma) and 1% SDS and incubated for 30 min at 37°C to block further oxidation of cysteine residues (19). The proteins were separated by SDS-PAGE and transferred to polyvinylidene fluoride (PVDF) membranes. The membranes were blocked with 5% skim milk in PBS and incubated with primary antibodies overnight at 4°C. Anti-NP1 (1:1000, Abcam), anti-MICAL3 (1:1000, Millipore or 1:200, H-56, Santa Cruz Biotechnology), anti-Numb (C29G11, 1:1000, Cell Signaling), anti-CRMP2 (C4G, 1:100, IBL) or anti-GAPDH (D23H3, 1:5000, Millipore) were used as primary antibodies. After washing three times in PBS containing 0.1% Tween 20, the PVDF membranes were incubated with horseradish peroxidase (HRP)-conjugated anti-rabbit or anti-mouse IgG as secondary antibodies at room temperature for 1 hr. Signals were developed

using an Immobilon Western Chemiluminescent HRP Substrate (Millipore) and examined using a LAS3000 (Fujifilm, Tokyo, Japan) imaging system. Intensity of each band was analyzed using ImageJ.

### **Immunofluorescence**

Formalin-fixed and paraffin-embedded breast cancer tissues were conducted on surgically resected breast carcinoma specimens from Kanazawa Medical University Hospital. Antigen retrieval was performed by heat induction in citrate buffer pH 6 after deparaffinization. After blocking for 1 hr at RT in normal serum (Dako), slides were incubated overnight in a humidified chamber at 4 °C with anti-NP1 (1:100, abcam) or Anti-Numb (1:100, abcam ab4147) antibodies. After washing with PBS, cells were incubated with Alexa 488 anti-rabbit or Alexa 546 anti-goat IgG antibodies as a secondary antibody at room temperature for 1 hr. Cells were coverslipped using glycerol containing DAPI (Sigma) to stain the nuclei and examined under a BZ9000 (Keyence).

Cultured cells were fixed in 4% paraformaldehyde/PBS (Nacalai Tesque) at room temperature (24°C) for 15 min. After washing in PBS containing 0.15% Triton X-100 for 10 min, cells were incubated with 1% bovine serum albumin (Nacalai Tesque) at room temperature for 60 min to block non-specific binding and then incubated with the primary antibody at 4°C overnight. Anti-MICAL3 (H-56, 1:50, Santa Cruz Biotechnology), Anti-CRMP2 (C4G, 1:50, IBL), Anti-Numb (1:100, Abcam 14140) or anti- $\alpha$ -Tubulin (DM1A, 1:200, Millipore) were used as primary antibodies. After washing with PBS, cells were incubated with an Alexa 546 anti-mouse IgG antibody as a secondary antibody at room temperature for 1 hr. Cells were coverslipped using glycerol containing DAPI (Sigma) to stain the nuclei and examined under a fluorescence microscope (Carl Zeiss).

### **In situ PLA**

For the analysis of interactions with proteins, the Duolink® *in situ* Proximity Ligation Assay (Olink Bioscience) was used. Cells were fixed in 4% paraformaldehyde/PBS and washed with PBS containing 0.15% Triton X-100 to permeabilize the cells. Cells were incubated overnight with the primary antibodies. After washing with PBS, both Probe marker PLUS (positive oligonucleotide) and MINUS (negative complementary oligonucleotide) were used as secondary antibodies. A detection reagent (red or green) was used to visualize protein interactions. The total number of signal dots was counted separately in the nucleus and the cytoplasm using a fluorescence microscope and analyzed using ImageJ.

### **Xenografts**

Eight-week-old female immunodeficient NSG mice were anesthetized with isoflurane (Abbott Japan). Ninety-day release  $\beta$ -estradiol (E2) pellets containing 0.72 mg E2 (Innovative Research of America) were implanted subcutaneously into the back of the neck 3 days before cell implantation. For PDX, breast cancer tissues obtained from breast cancer patients were cut into 1-mm squares, and five pieces were suspended in Matrigel (BD Biosciences) to produce 50  $\mu$ l of the cell mixture. Five pieces per site, or cells expressing the indicated constructs, were subsequently injected into the mammary fat pads of NSG mice. When tumors reached >100 mm<sup>3</sup>, the mice were killed. To distinguish between the human tumor cells and mouse cells in PDX, FITC-labeled anti-mouse H-2Kd was used to label mouse major histocompatibility class I, and concurrently, V450-labeled anti-rat CD45 (BD Pharmingen) was used to label mouse leukocytes. The population excluding H-2Kd and CD45-positive cells was isolated using flow cytometry. Tissue fragments were retransplanted into another cohort of mice. For limiting dilution assays (LDAs), cells were suspended in 50  $\mu$ l Matrigel (BD Biosciences) and injected subcutaneously into the mammary fat pad of NSG mice.

### **qRT-PCR**

Total RNA was prepared using the TRIzol Reagent (Invitrogen) and was transcribed into cDNA using a High Capacity cDNA Reverse Transcription kit (Applied Biosystems). qRT-PCR was performed using TaqMan probes from Applied Biosystems, according to the manufacturer's recommendations.

### **H<sub>2</sub>O<sub>2</sub> assay**

The Amplex red hydrogen peroxide/peroxidase assay kit (Invitrogen) was used to measure H<sub>2</sub>O<sub>2</sub> production (30). HEK293FT cells ( $1 \times 10^6$  cells) transfected with GFP-fusion constructs were lysed using 120  $\mu$ l lysis buffer containing 20 mM HEPES (pH 7.4), 100 mM NaCl, 1% NP-40, and Protease Inhibitor Cocktail. After incubation at 4°C, lysates were cleared by centrifugation. Reactions were performed in a 100- $\mu$ l volume consisting of 50  $\mu$ l cell lysate, 200  $\mu$ M NADPH, Amplex red reagent (10-acetyl-3,7-dihydroxyphenoxazine), and 0.1 U/ml HRP in reaction buffer. The positive control was 1  $\mu$ M H<sub>2</sub>O<sub>2</sub>. Absorbance at 560 nm was measured using a Wallac Victor 1420 multilabel counter.

### **Tissue Microarrays**

We used breast cancer tissue microarrays (HBre-Duc150Sur-01) that were purchased from Biomax Inc. (<http://www.biomax.us/>). Tissue microarrays included 150 primary breast cancer cases (<https://www.biomax.us/tissue-arrays/Breast/HBre-Duc150Sur-01>). The demographic and clinicopathological details of patients and tumors are provided on the manufacturer's website. Immunohistochemical evaluation of NP1 (1:800, Abcam 81321) and Numb (1:5,000, Abcam 4147) was performed by a pathologist (H.M.) based on light microscopic observations. Area score was recorded as the percentage of positive tumor cells by increments of 5 %.

### **Statistics**

The Student's unpaired *t*-test was used to compare differences between two samples, and values of  $p < 0.05$  were considered significant. Values are presented as means  $\pm$  SD. For the sphere assay, the spheres were counted, and the percentage of sphere-forming cells was determined for each group. LDAs of frequency determinations, as well as the corresponding *p* values, were generated using ELDA software, which took into account whether the assumptions for LDA were met (<http://bioinf.wehi.edu.au/software/elda/index.html>, provided by the Water and Eliza Hall Institute) (SI ref. 1). The *p*-values for multiple testing were obtained using the method of Holm. For the Kaplan-Meier analysis, *p*-value was calculated by using the log-rank test.

### **Acknowledgements**

We are grateful to H. Miyoshi for providing the lentivirus vector and to A. Akhmanova for providing MICAL3 cDNA constructs. We thank H. Nakauchi, Y. Ishii, and A. Fujita for their help with flow cytometry and A. Nakayama and Y. Tanabe for immunohistochemistry. This work was supported in part by an Extramural Collaborative Research Grant from the Cancer Research Institute, Kanazawa University, Hokkoku Gan-Kikin, a Grant-in-Aid for Scientific Research on Innovative Areas from MEXT (22130009), a Grant-in-Aid for Scientific Research from JSPS (15H04294, 17K19587 and 18H02679), and a research grant from AMED Project for Development of Innovative Research on Cancer Therapeutics,

Project for Cancer Research and Therapeutic Evolution (16cm0106120h0001) and Practical Research for Innovative Cancer Control (16ck0106194h0001) to N. Gotoh. This work was supported in part by a Grant-in-Aid for JSPS Fellows (14J05402 and 16J40231) to K. Tominaga.



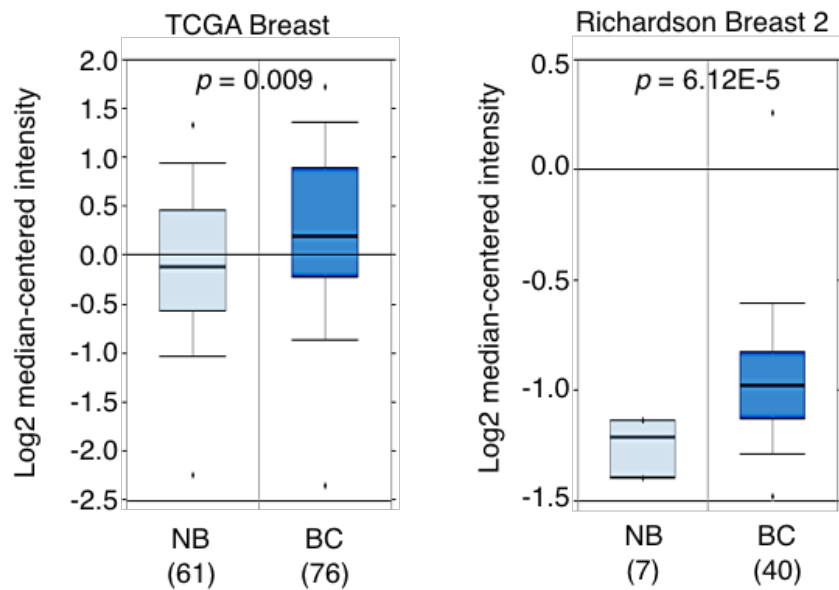


**Fig. S1.** *NPI* expression was higher in breast cancer tissues (BC) than in normal breast tissues (NB) in Oncomine cancer gene expression database (Right; TCGA Breast, Left; Richardson Breast 2) P-values were calculated by Student's t-test.

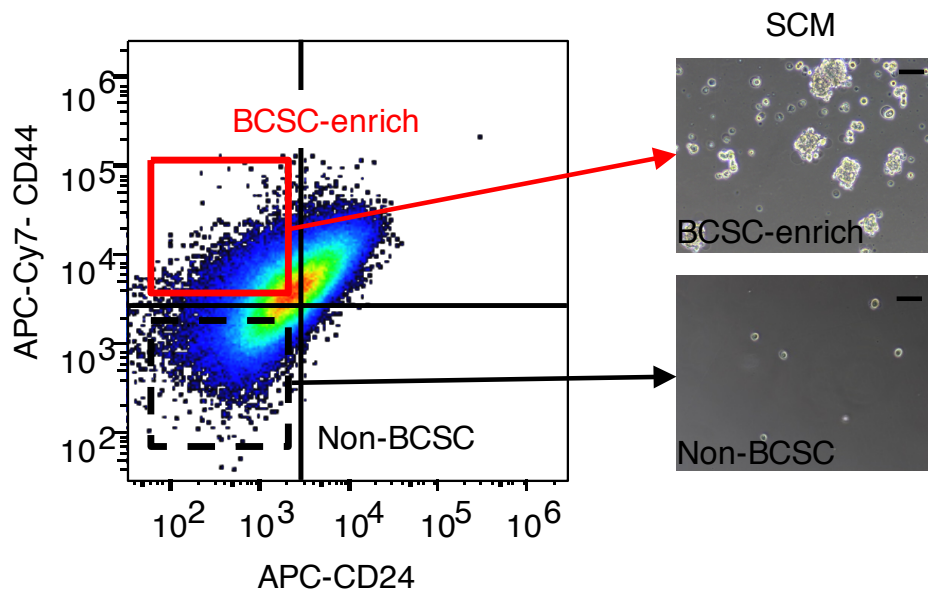


**Fig. S2.** The tumor spheres formation in  $CD24^{-low}/CD44^{high}$  cell population (BCSC-enrich) but not in the other cell population (Non-BCSC) in patient-derived breast cancer cells (Patient #10).

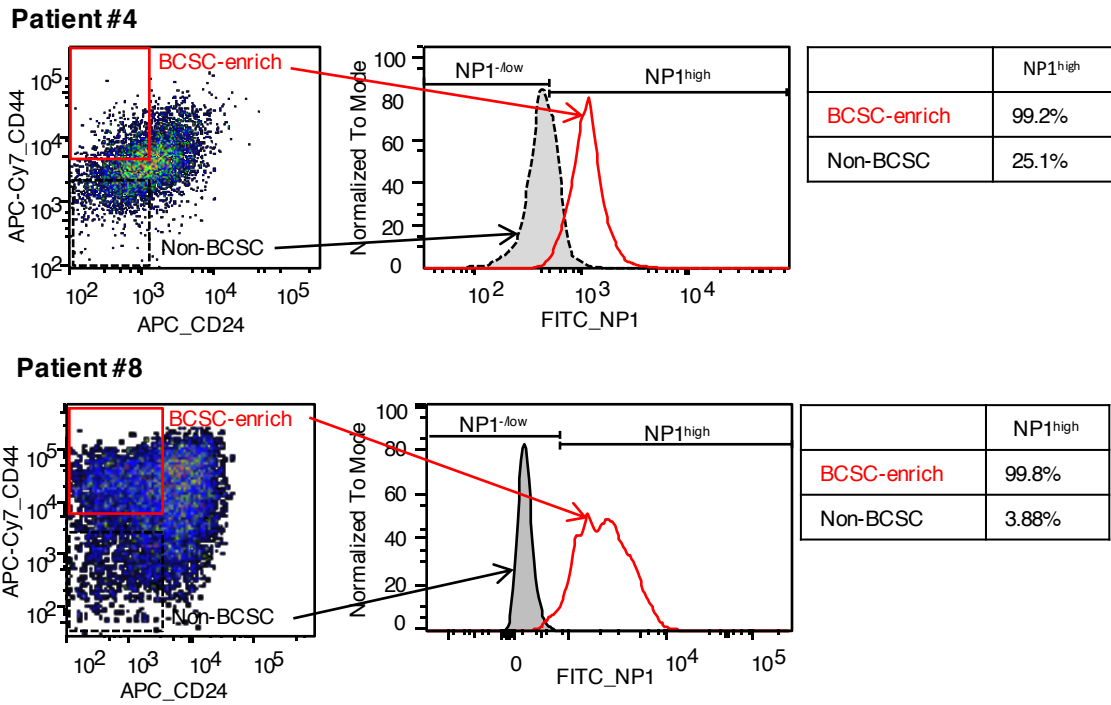


**Fig. S3.** NP1 is predominantly expressed in BCSC-enriched population. FACS analysis of freshly obtained patient-derived BCCs (upper; Patient #4, lower; Patient #8). The cells were sorted according to the expression of CD44 and CD24. The CD44<sup>high</sup>/CD24<sup>low</sup> BCSC-enriched population and the other population were then sorted according to the expression of NP1.

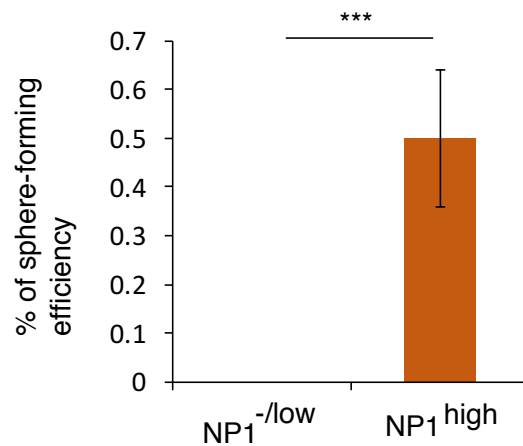


**Fig. S4.** The NP1<sup>high</sup> cell population, but not the NP1<sup>-/low</sup> cell population, gave rise to tumor spheres in SCM. NP1<sup>high</sup> cells but not NP1<sup>-/low</sup> cells of patient-derived BCCs (Patient #1) formed tumor spheres in SCM.  $n = 4$ . Data are shown as Mean  $\pm$  SD. P-value was calculated by Student's t-tests. \*\*\* $p < 0.001$ .

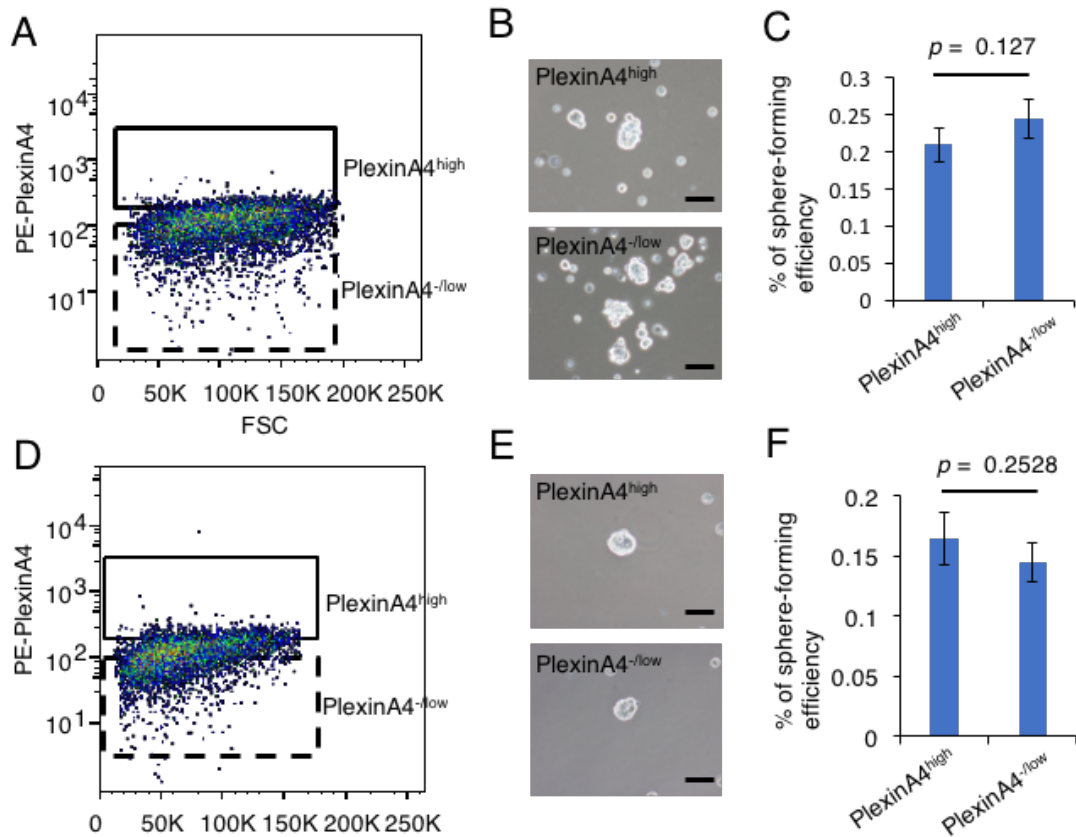


**Fig. S5.** The expression of Plexin A4, a coreceptor for Sema3 signaling, is not involved in tumor sphere formation (A-C, Patient #4; D-E, Patient #8). (A and D) FACS analysis of freshly obtained patient-derived BCCs. The cells were sorted according to the expression of Plexin A4. (B and E) Representative phase contrast images of tumor sphere formation in patient-derived BCCs in SCM. Scale bar: 100  $\mu$ m. (C and F) Quantification of the tumor sphere-forming activity of patient-derived BCCs in SCM.  $n = 4$ . Data are shown as Mean  $\pm$  SD. P-value was calculated by Student's t-tests.

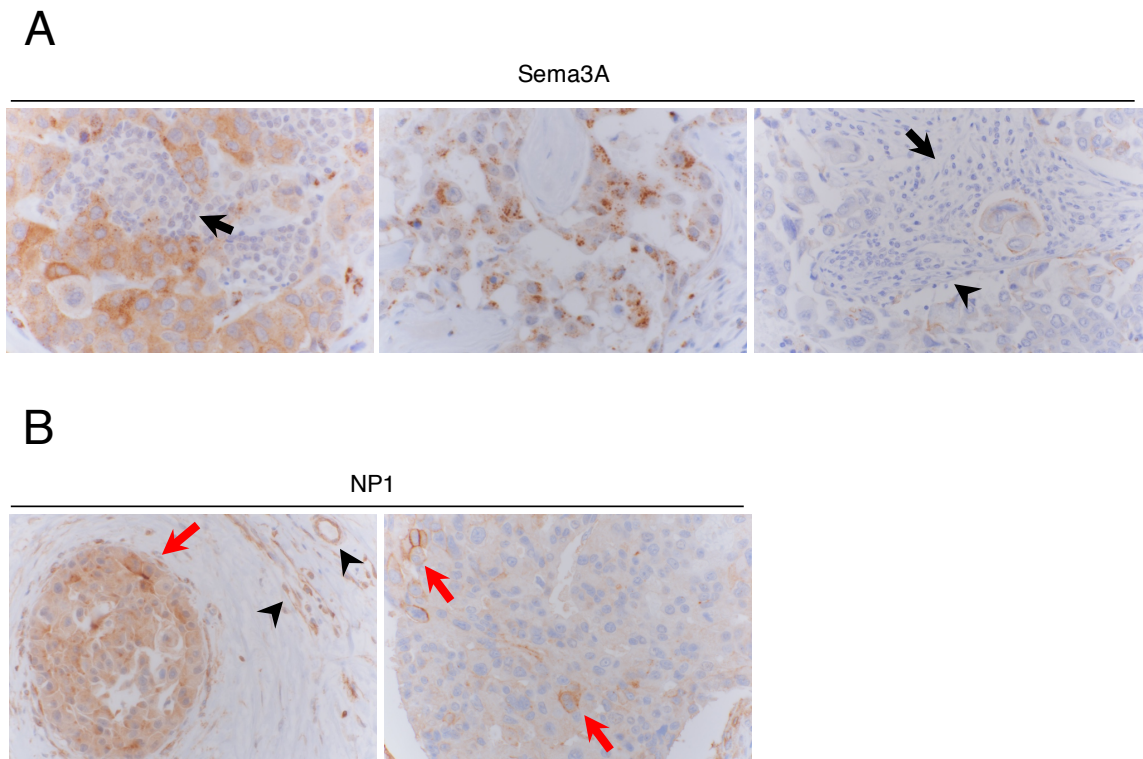


**Fig. S6.** Immunohistochemical staining of Sema3A (A) and NP1 (B) in breast cancer tissues (triple negative type). Original magnification; 400x. Black arrowheads; endothelial cells, Black arrows; lymphocytes, Red arrows; NP1 positive cells in the cell membrane in tumor cells. While patchy or granular cytoplasmic staining of tumor cells was observed with antibody against Sema3A, no detectable protein was observed in endothelial cells or stroma of tumors. With antibody against NP1, we observed a few tumor cells with strong staining in the cell membrane and weak or modest staining in the cytoplasm, while others had not-so-obvious staining in the cell membrane and staining intensities were variable in the cytoplasm. We observed positive staining in endothelial cells, but not in stroma of tumors.

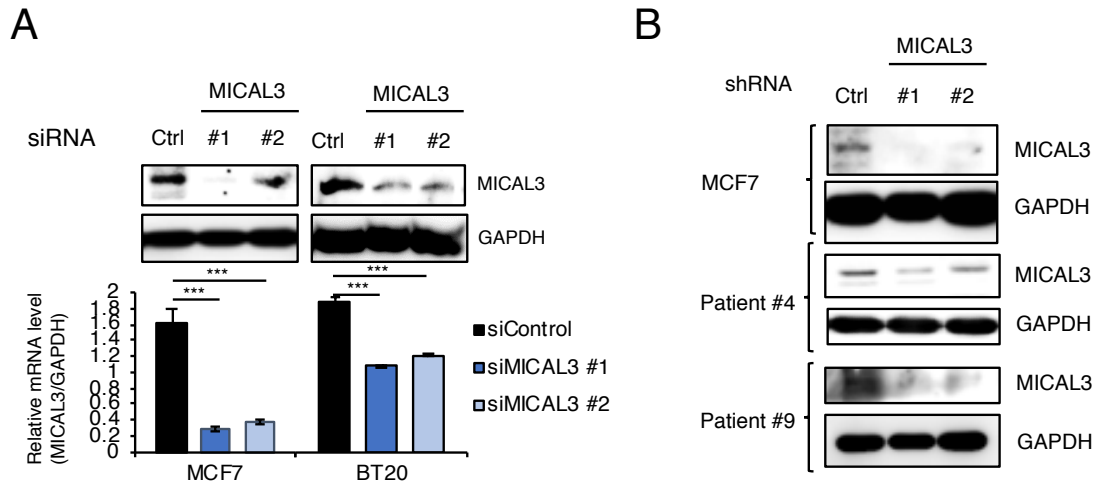


**Fig. S7.** *MICAL3* knockdown in breast cancer cells. (A) Expression of *MICAL3* protein by Immunoblotting (upper) and *MICAL3* mRNA by qRT-PCR (lower) in MCF7 cells or BT20 cells transiently transfected with control or *MICAL3* siRNA (individual siRNAs). Ctrl, control siRNA.  $***p < 0.001$  by the Student's t-test. mean  $\pm$  SD of triplicate. (B) Expression of *MICAL3* protein by immunoblotting for MCF7 cells and patient-derived BCCs transduced with control (Ctrl) or *MICAL3* shRNA.  $n = 4$ . Data are shown as Mean  $\pm$  SD. P-value was calculated by Student's t-tests.  $***p < 0.001$ .

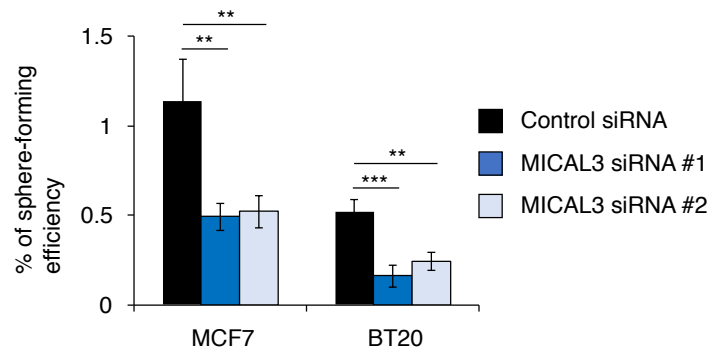
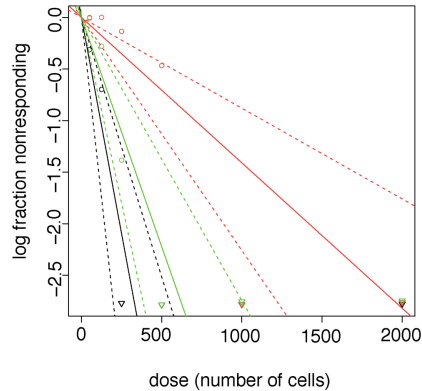


**Fig. S8.** Sema3A-induced tumor sphere formation was significantly decreased by *MICAL3* knockdown in BCCs. Sema3A-induced tumor sphere formation was decreased by *MICAL3* knockdown in MCF7 or BT20 cells.  $n = 4$ . Data are shown as Mean  $\pm$  SD. P-value was calculated by Student's t-tests.  $**p < 0.01$ ,  $***p < 0.001$ .

Patient #4

Cells/well	2,000	1,000	500	250	125	50	<i>p</i> value vs Control	1/stem cell frequency (Lower-Upper)
Control shRNA	8/8	8/8	8/8	8/8	4/8	2/8		119 (199-71.7)
MICAL3 shRNA #1	8/8	8/8	3/8	1/8	0/8	0/8	1.43E-06	709 (1137-443.7)
MICAL3 shRNA #2	8/8	8/8	8/8	6/8	2/8	0/8	0.0909	225 (364-139.2)



Patient #9

Cells/well	2,000	1,000	500	250	125	50	<i>p</i> value vs Control	1/stem cell frequency (Lower-Upper)
Control shRNA	8/8	8/8	8/8	4/8	0/8	0/8		327 (524-204)
MICAL3 shRNA #1	8/8	6/8	2/8	0/8	0/8	0/8	0.00133	1065 (1752-647)
MICAL3 shRNA #2	8/8	5/8	4/8	1/8	0/8	0/8	0.00421	919 (1494-566)

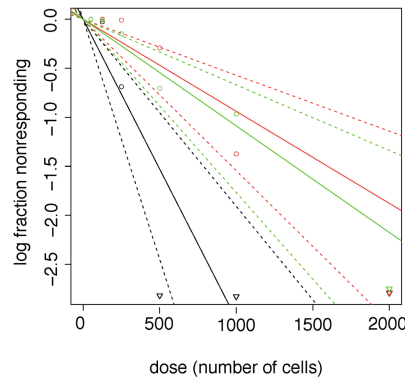


**Fig. S9.** *In vitro* limiting dilution assay for *MICAL3* knockdown cells in patient-derived BCCs. 2,000, 1,000, 500, 250, 125 or 50 cells were seeded into 96-well ultra-low attachment plates and cultured in a floating condition in SCM (upper; Patient #4, lower; Patient #9). Results were obtained 7 days after seeding. The sphere-forming activity was significantly decreased in *MICAL3* knockdown cells in each patient-derived BCCs. Frequency determinations were generated using ELDA software (SI Ref. 1). P-values are adjusted for multiple testing using the method of Holm.

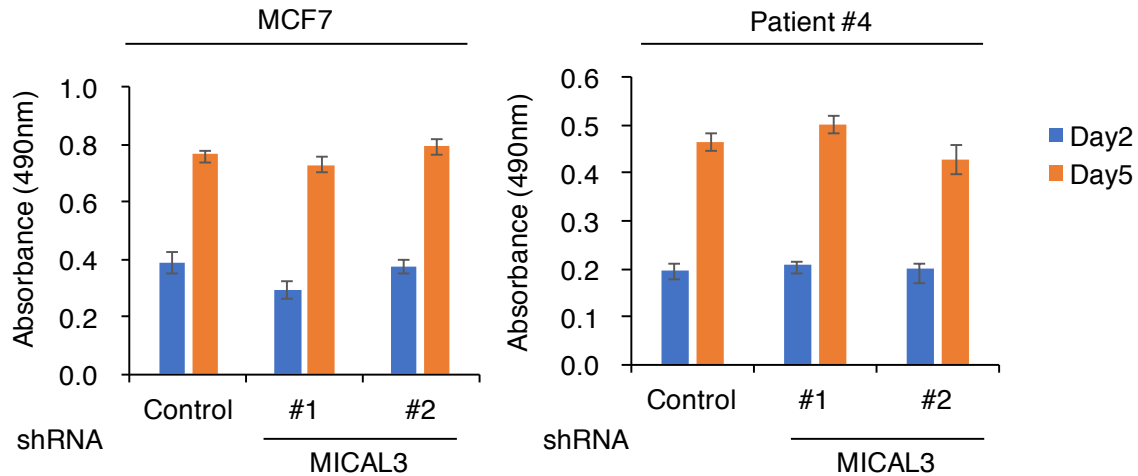


**Fig. S10.** *MICAL3* knockdown did not affect cell proliferation in MCF7 cells and patient-derived BCCs. Cells were cultured in an adherent condition in 10% serum-containing medium. MTT assay was performed on day 2 and day 5.  $n = 4$ . Data are shown as Mean  $\pm$  SD.

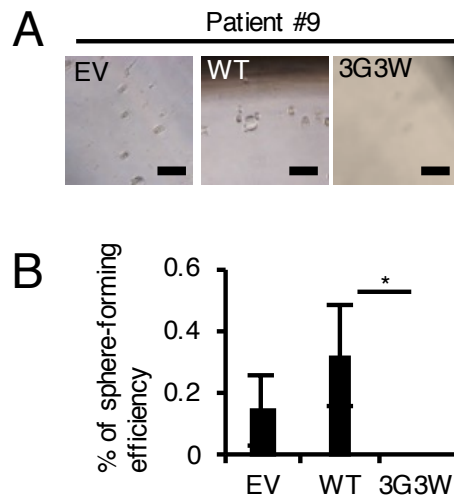


**Fig. S11.** MO domain of *MICAL3* plays critical roles in tumor sphere formation. (A) Representative phase contrast images of tumor sphere formation by patient-derived BCCs transiently transfected with the indicated constructs cultured in SCM. Scale bar: 100  $\mu$ m. (B) Tumor sphere formation by patient-derived BCCs transfected with the indicated constructs cultured in SCM.  $n = 4$ . Data are shown as Mean  $\pm$  SD.  $*p < 0.05$  by the Student's t-tests.

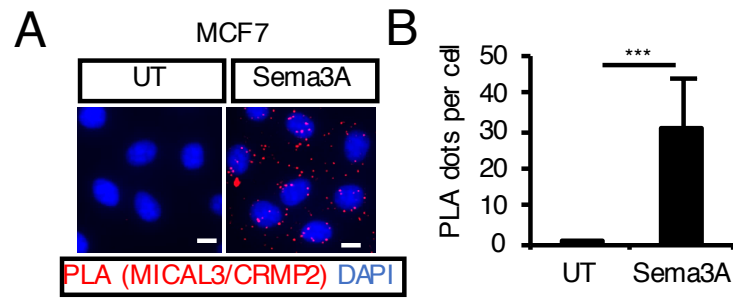


**Fig. S12.** The number of PLA dots was greatly increased in Sema3A-containing medium. (A) In situ PLA showed interactions between MICAL3 and CRMP2 in MCF7 cells treated with 200 ng/ml Sema3A for 24 hr. PLA dots (red) indicate the interaction between MICAL3 and CRMP2 by immunofluorescence. Nuclei were stained with DAPI. UT, untreated. Scale bar: 40  $\mu$ m. (B) Quantification of the number of PLA dots per cell. One hundred cells were counted for each condition. UT, untreated. Data are shown as Mean  $\pm$  SD. \*\*\* $p < 0.001$  by the Student's t-tests.



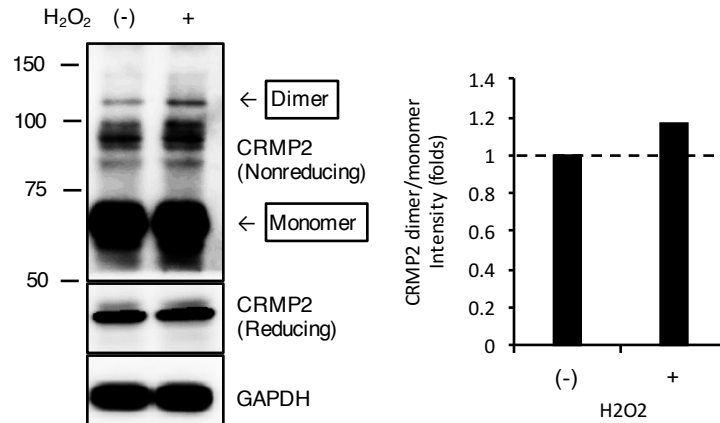


**Fig. S13.** Dimerization of CRMP2 was induced by treatment with H<sub>2</sub>O<sub>2</sub>. (Left) Expression of CRMP2 protein in MCF7 cells was analyzed by immunoblotting following treatment with or without 1 μM H<sub>2</sub>O<sub>2</sub> for 15 min. Cell lysates were immunoblotted with anti-CRMP2 antibodies under non-reducing conditions (upper panel). Upper arrow indicates homodimers of CRMP2 and lower arrow indicates monomers of CRMP2. Reducing condition was assayed as a positive control. GAPDH was the loading control. (Right) The normalized intensity of CRMP2 homodimers was obtained from MCF7 cells following treatment with or without 1 μM H<sub>2</sub>O<sub>2</sub>.

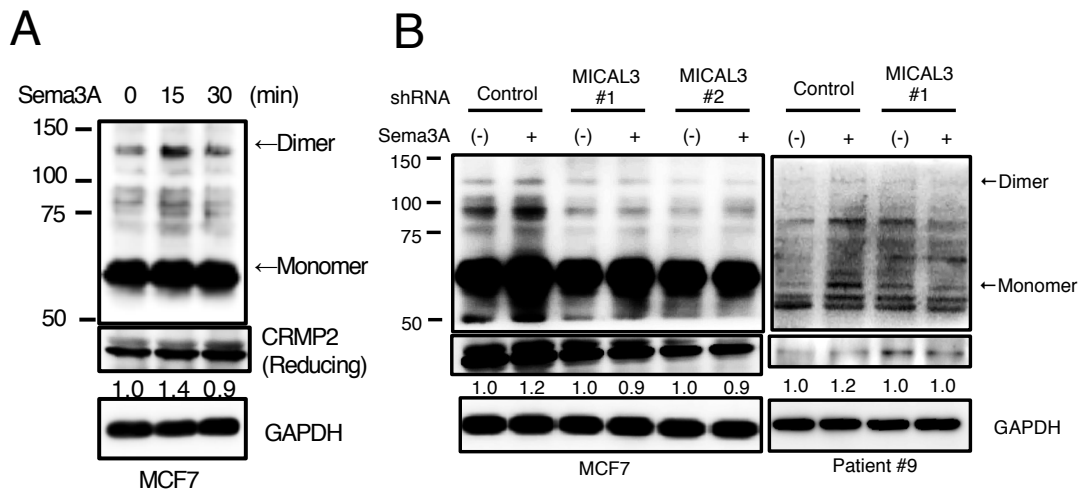


**Fig. S14.** Dimerization of CRMP2 was induced by treatment with Sema3A. (A) Immunoblotting analysis of the expression of CRMP2 in MCF7 cells following stimulation with or without 200 ng/ml Sema3A. (B) Immunoblotting analysis of the expression of CRMP2 in MCF7 cells or patient-derived BCCs transduced with control or *MICAL3* shRNA and stimulated with or without 200 ng/ml Sema3A for 15 min. Upper arrow indicates homodimers of CRMP2 and lower arrow indicates monomers of CRMP2. Reducing condition was assayed as a positive control. In figures, GAPDH was the loading control. Intensities of the bands were calculated using Image J software and normalized to CRMP2 monomer expression levels.

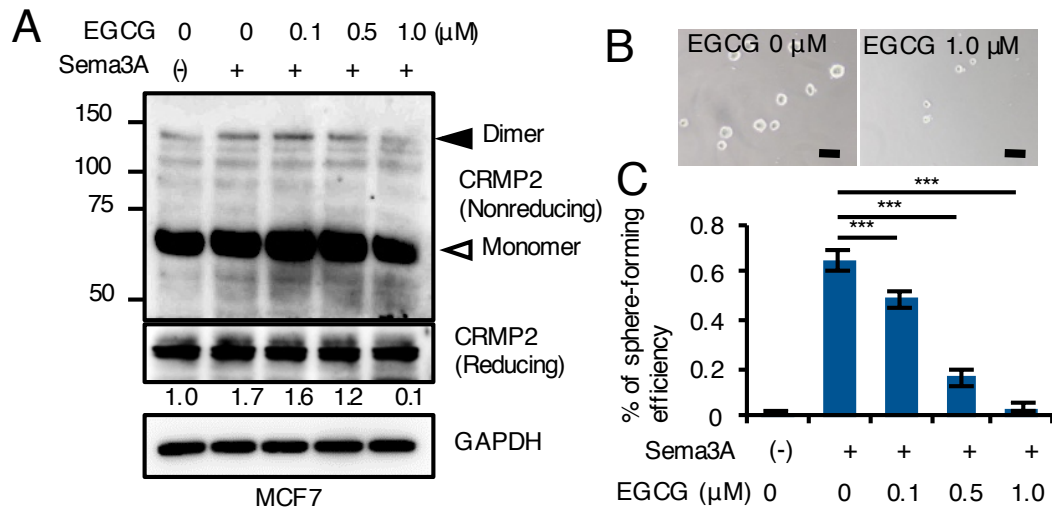


**Fig. S15.** EGCG-treatment decreased Sema3A-induced dimerization of CRMP2 and tumor sphere formation. (A) Immunoblotting analysis of the expression of CRMP2 in MCF7 cells stimulated with or without 200 ng/ml Sema3A and EGCG at the indicated concentrations for 15 min. (B) Representative phase contrast images of tumor sphere formation by MCF7 cells in the presence or absence of EGCG in Sema3A-contained medium. Scale bar: 100 μm. (C) Quantification of the Sema3A-induced tumor spheres of MCF7 cells with EGCG at the indicated concentrations.  $n = 4$ . In figures, GAPDH was the loading control. Intensities of the bands were calculated using Image J software and normalized to CRMP2 monomer expression levels. Data are shown as Mean  $\pm$  SD. \*\*\* $p < 0.001$  by the Student's t-tests.

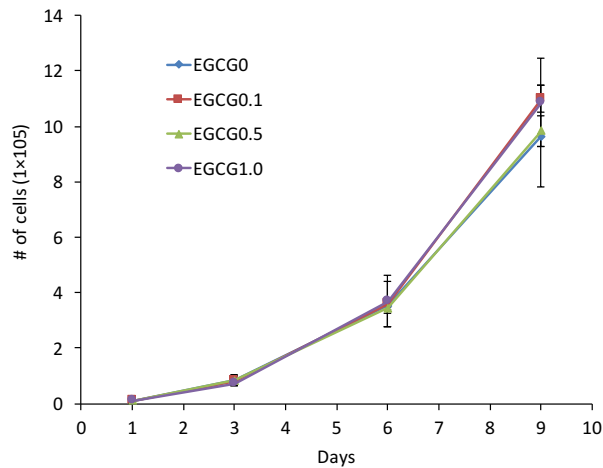


**Fig. S16.** EGCG-treatment did not affect cell proliferation in MCF7 cells. Cells were cultured in 10% serum-containing medium in the presence (0.1, 0.5, or 1.0  $\mu$ M) or absence of EGCG, and number of cells was calculated at the indicated dates.  $n=3$ . Data are shown as Mean  $\pm$  SD.

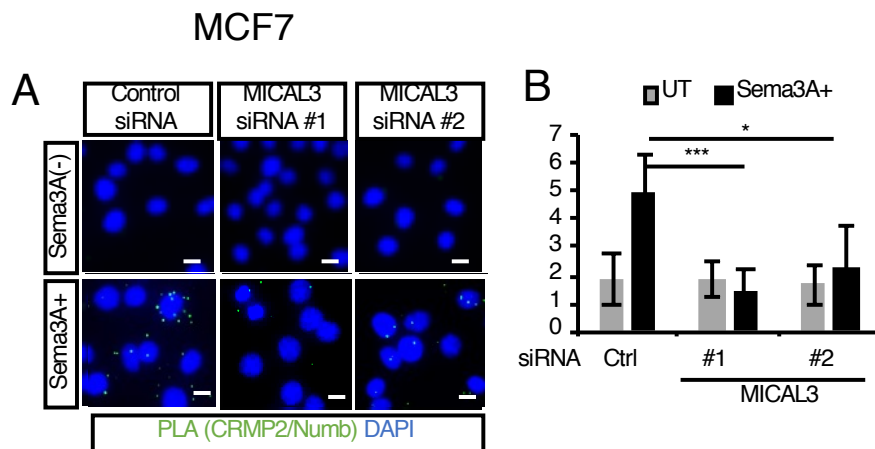


**Fig. S17.** *MICAL3* knockdown significantly decreased Sema3A-induced interaction between CRMP2 and Numb. (A) In situ PLA showed interactions between CRMP2 and Numb in NP1 positive MCF7 cells with 200 ng/ml Sema3A treatment for 24 hr. PLA dots (green) indicate the interaction between CRMP2 and Numb by immunofluorescence. Nuclei were stained with DAPI. The interaction was decreased by knockdown of *MICAL3*. Scale bar: 40  $\mu$ m. (B) Quantification of the number of PLA dots per cell as shown in (A). One hundred cells were counted for each condition. UT, untreated; Ctrl, control siRNA. Data are shown as Mean  $\pm$  SD. \* $p < 0.05$ , \*\*\* $p < 0.001$  by the Student's *t*-tests.

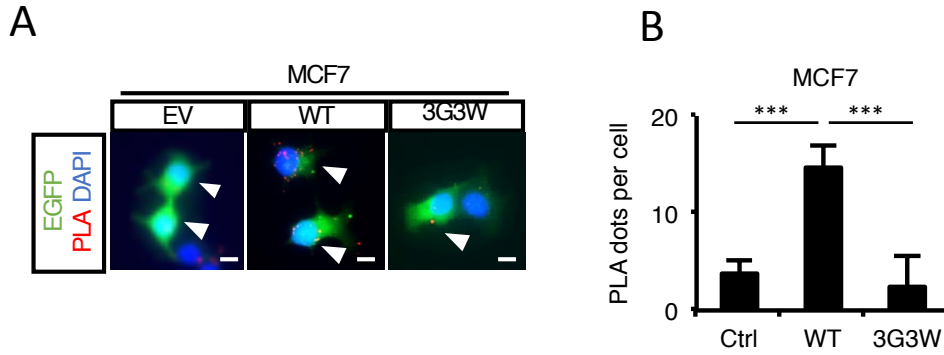


**Fig. S18.** MO domain of MICAL3 is required for the interaction between CRMP2 and Numb. (A) The interaction between CRMP2 and Numb was greater in MICAL3-WT-transfected cells than in MICAL3-3G3W-transfected cells or vector-transfected cells (EV) with Sema3A treatment for 24 hr. White arrowheads indicate EGFP-positive cells. PLA dots (red) indicate the interaction between CRMP2 and Numb by immunofluorescence. EV, empty vector. Scale bar, 100  $\mu$ m. (B) Quantification of the number of PLA dots per cell. Twenty cells were counted for each condition. Data are shown as Mean  $\pm$  SD.

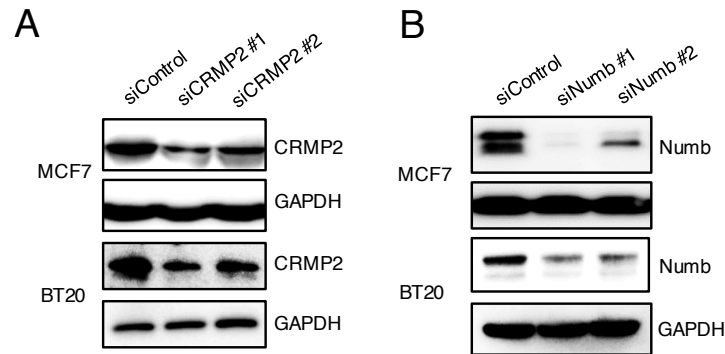


**Fig. S19.** *CRMP2* or *Numb* knockdown in breast cancer cells. (A) Expression of CRMP2 protein was examined by immunoblotting using the lysate of MCF7 or BT20 cells transiently transfected with control or *CRMP2* siRNA (individual siRNAs). (B) Expression of Numb protein was examined by immunoblotting using the lysate of MCF7 or BT20 cells transiently transfected with control or *Numb* siRNA (individual siRNAs). GAPDH was the loading control.

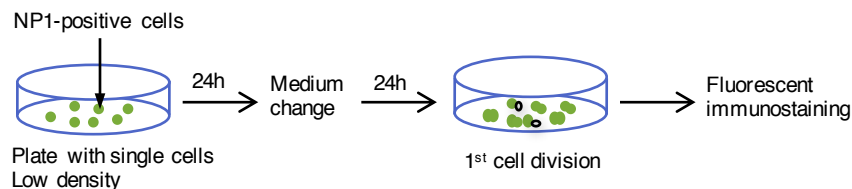


**Fig. S20.** A schematic of the cell pair assay using patient-derived breast cancer cells. Single cells were plated at low density. After 24 hr, medium was changed to the medium with or without Sema3A.

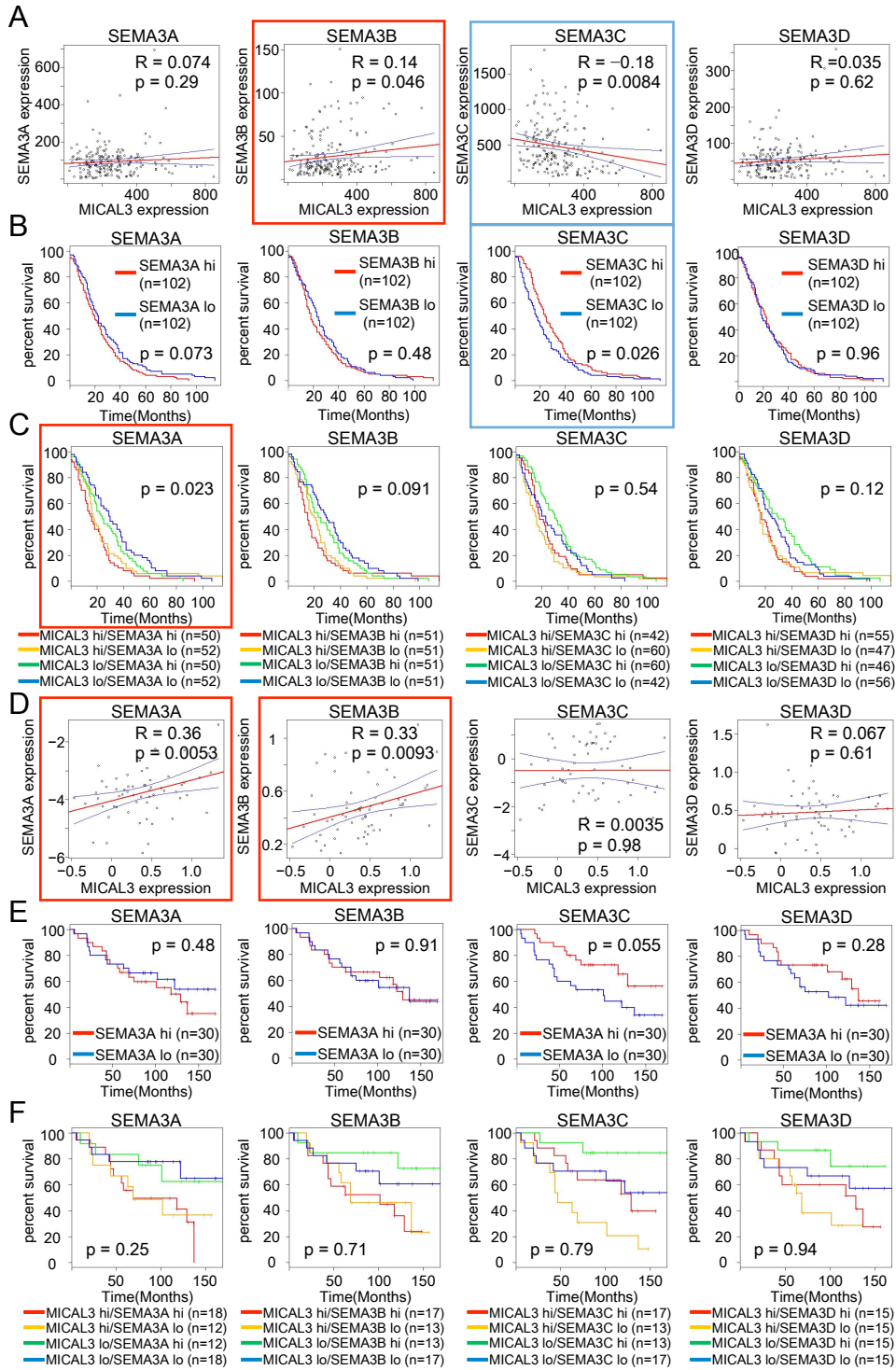


**Fig. S21.** Expression levels of NP1 ligands, i.e. semaphorins, and their co-expression with *MICAL3* in gene expression profiles of breast cancer samples. (A, D) Correlation between *Sema3A*, *Sema3B*, *Sema3C*, or *Sema3D* and *MICAL3* expression in gene expression profiles. (B, E) Kaplan-Meier analysis of the relapse-free survival of patients with breast cancer tissues showing low or high *Sema3A*, *Sema3B*, *Sema3C*, or *Sema3D* expression alone. The median

was used for determining the cut-off values. (C, F) Kaplan-Meier analysis of the relapse-free survival of patients with breast cancer tissues showing low or high combined expression levels of *Sema3A*, *Sema3B*, *Sema3C*, or *Sema3D* and *MICAL3*. The median was used for determining the cut-off values. The gene expression profiles GSE1379 (A-C) and GSE12276 (D-E) were used for analysis.

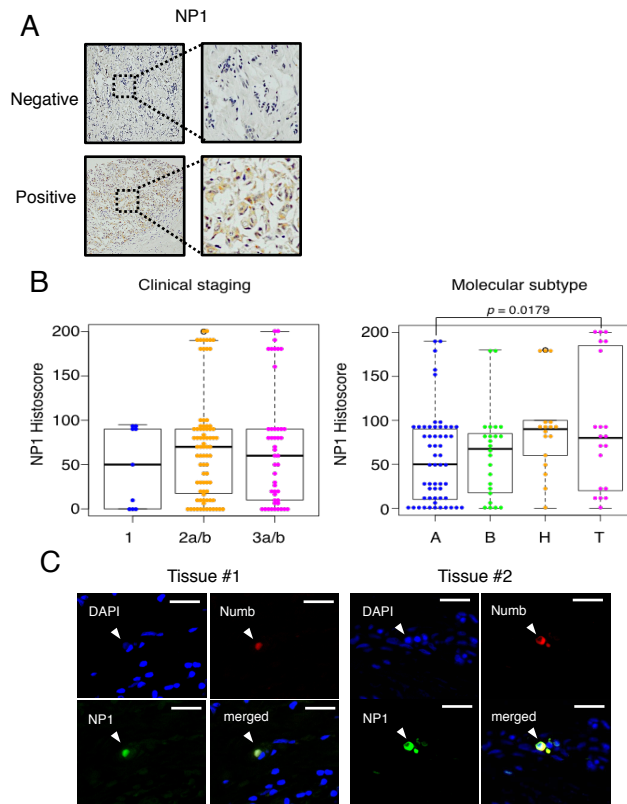


**Fig. S22.** Expression of NP1 in human breast cancer tissues. (A) Immunohistochemical staining of breast cancer tissue microarray using an antibody against human NP1. Scale bar: 100  $\mu\text{m}$ . (B) Quantification of NP1 expression levels in a tissue microarray as a function of the different tumor stages (left panel) and different subtypes (right panel). A, luminal A; B, luminal B; H, HER2-enriched; T, triple negative subtype.  $n = 134$ . Multiple comparisons of the data were performed by ANOVA with Dunnett's test. (C) Immunofluorescence staining of two breast cancer tissues (triple negative type) using antibodies against NP1 and Numb. White arrowheads indicate double positive cells. Scale bar: 40  $\mu\text{m}$ .

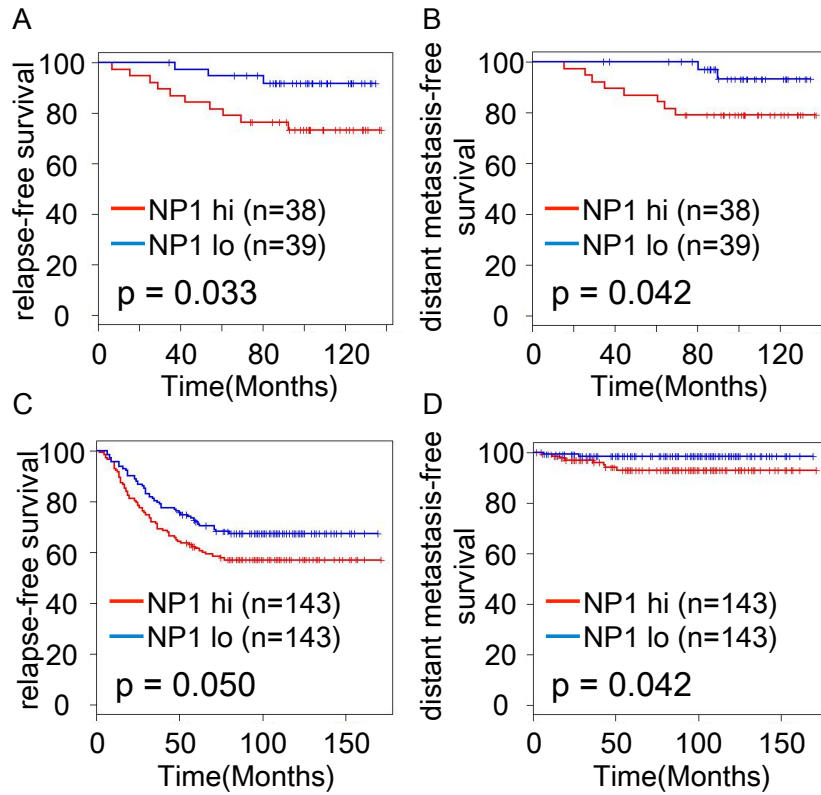


**Fig. S23.** High levels of *NP1* expression in human breast cancer tissues are associated with worse outcomes. Kaplan-Meier analysis of the relapse-free survival (A, C) or distant metastasis-free survival (B, D) of patients with breast cancer tissues showing low or high *NP1* expression. The median was used for determining the cut-off values. The gene expression profiles GSE9195 (A, B) and GSE2034 (C, D) were used for analysis.

**Table S1. Characteristics of breast cancer patients in this study**

<b>Patient #</b>	<b>Diagnosis</b>	<b>ER</b>	<b>PgR</b>	<b>HER2</b>	<b>pStage</b>	<b>Molecular Subtype</b>
<b>1</b>	Invasive ductal ca.	100%(+)	100%(+)	2+	IIA	Luminal A
<b>2</b>	Invasive papillotubular ca.	100%(+)	80%<(+) )	2+	I	Luminal A
<b>3</b>	Invasive ductal ca.	+	+	2+	I	Luminal A
<b>4</b>	Squamous cell ca.	-	-	0	IIB	TN
<b>5</b>	Invasive lobular ca.	40%(+)	1%(+)	1+	III	Luminal B
<b>6</b>	Invasive ductal ca.	3+	3+	1+	IIA	Luminal A
<b>7</b>	Invasive papillotubular ca.	-	-	1+	IIIA	TN
<b>8</b>	Scirrhou s ca.	3+	3+	0	III	Luminal A
<b>9</b>	Invasive lobular ca.	1+	-	2+	IV	Luminal B
<b>10</b>	Ductal ca. in situ	10%(+)	-	3+	0	Luminal B

ca; carcinoma, TN; triple negative type.



**Table S2. The target sequences of MICAL3 shRNA plasmids.**

shRNA	Sequence
Control	5'-GATCCCGTGTGCTTTGTAGGGTTCTACGTGTGCTGTCCGTAGAATCCTACAAAGCGCGCTTTTGGAAAT-3' 5'-CTAGATTTCAAAAAGCGCGCTTTGTAGGATTCGACGGACAGCACACGTAGAACCTACAAAGCACACGGG-3'
MICAL3 isoform 1 #1	5'-GATCCCGATGTGCGCTGGACTCGTATAACGTGTGCTGTCCGTTATATGAGTCCAGTGACACGTCTTTTGGAAAT-3' 5'-CTAGATTTCAAAAAGACGTGCACTGGACTCATATCACGGACAGCACACGTTATACGAGTCCAGCGCACATCGGG-3'
MICAL3 isoform 1 #2	5'-GATCCCGGGAGTTCCTCCGACATGGAACGTGTGCTGTCCGTTTTCATGTTGGAGGAGCTCCCTTTTGGAAAT-3' 5'-CTAGATTTCAAAAAGGGAGCTCCTCCAACATGAAGACGGACAGCACACGTTTCCATGTCGGAGGAACCTCCGGG-3'

**Table S3. The target sequences of MICAL3 siRNAs.**

siRNA (ON-TARGETplus)	Target Sequence
MICAL3 #1	5'-CCAAGAGAAUGAACGGUAU-3'
MICAL3 #2	5'-CCGUACAGCCAUCGACUUA-3'

**Table S4. The target sequences of CRMP2 siRNAs and Numb siRNAs**

siRNA (Stealth <sup>TM</sup> RNAi)	Sequence
CRMP2 #1	5'-GGGUAAAUUCUUCUCGUGUACAU-3' 5'-AUGUACACGAGGAAGAAUUUACCC-3'
CRMP2 #2	5'-GCUCUCAAAGAUCGCUUCCAGCUAA-3' 5'-UUAGCUGGAAGCGAUCUUUGAAAGC-3'
NUMB #1	5'-GACCGAUGGUUAGAAGAGGUGUCUA-3' 5'-UAGACACCUCUUCUAACCAUCGGUC-3'
NUMB #2	5'-GAGAAAGAAGGAUGUUUAUGUCCA-3' 5'-UGGAACAUAAACAUCUUCUUCUC-3'

**SI Reference**

1. Hu Y, Smyth GK (2009) ELDA: Extreme limiting dilution analysis for comparing depleted and enriched populations in stem cell and other assays. *J Immunol Methods* 347(1–2):70–78.

